

Synthesis and structural characterization of undoped and Co doped zinc oxide thin films obtained by aerosol assisted chemical vapour deposition

P. Amézaga-Madrid, W. Antúnez-Flores, R.J. Sáenz-Hernández, R. Martínez-Sánchez, M. Miki-Yoshida.

Abstract

Dilute magnetic oxides are transparent, wide-bandgap materials that behave ferromagnetically when doped with a few percent of a magnetic 3d cation. They have attracted a great deal of interest due to the integration of semiconducting and magnetic properties in a material, that is a prerequisite for successful fabrication of useful devices for the emerging technologies of spintronics. Here we report a study of growth characteristics and microstructural properties of undoped and Co doped ZnO films grown onto borosilicate glass substrates, using aerosol assisted chemical vapour deposition method. The obtained films are single phase, of Wurtzite type, some of them with a strong *c*-axis orientation, i.e. with the *c*-axis normal to the substrate surface.

Keywords: Thin films, Vapour deposition, X-ray diffraction.

Introduction

Dilute magnetic oxides semiconductors are transparent, widebandgap materials that behave ferromagnetically when doped with a few percent of a magnetic 3d cation [1]. The phenomenon is observed in thin films and nanocrystals, but not in well-crystallized bulk material. They have attracted a great deal of interest due to the integration of semiconducting and magnetic properties in one material that is a prerequisite for successful fabrication of useful devices for the emerging technologies of spintronics [2].

<https://cimav.repositorioinstitucional.mx/jspui/>

There are several diluted magnetic semiconductors exploited, such as $\text{Ga}_{1-x}\text{Mn}_x\text{As}$, doped ZnO and doped TiO_2 . ZnO is one of the best candidates; it is optically transparent and has n or p type conductivity depending on the doping or co-doping technique [3]. Many studies were done on Co:ZnO films which were deposited either by pulsed laser deposition (PLD) using a KrF laser [4], a sol-gel method [5], radio-frequency magnetron co-sputtering [6], or spray pyrolysis [7]. In this work a study of structural and optical properties of undoped and Co doped ZnO films grown onto borosilicate glass substrates, using aerosol assisted chemical vapour deposition method. Deposition temperature was varied between 623 and 723K. Dopant concentration was fixed at 5 and 10 at.%. The microstructure of the films was characterized by X-ray diffraction, scanning electron microscopy and atomic force microscopy.

Experimental

Undoped and Co doped ZnO films were grown onto borosilicate 7059 (2.5cmx2.5 cm) glass substrates, using an aerosol assisted chemical vapour deposition (AACVD) set up similar to that previously reported [8]. The starting solution was a dilution of Zn acetate and Co acetate in methanol (99.9% pure); Co concentration was varied between 0 (for undoped) and 10 at.%. The films were prepared at different temperatures between 623 and 723K. An ultrasonic nebulizer (PG-24) working at 2.4MHz generated the aerosol that was conveyed by the carrier gas and directed towards the substrate by a nozzle, which had a periodic movement at constant velocity ($\sim 0.5\text{mms}^{-1}$) to scan the whole surface of the substrate. The total number of steps was

<https://cimav.repositorioinstitucional.mx/jspui/>

varied in order to obtain films of different thickness. Table 1 summarizes the principal deposition parameters used in this work.

X-ray diffraction (XRD) patterns were acquired to determine the crystalline phases present in the films. Patterns were obtained in a Bragg–Brentano geometry in an X-Pert system, using Cu K α radiation ($\lambda = 0.1542$ nm) at 40 keV and 30mA. The scanning angle 2θ was varied between 15° and 80° , at 0.1° step. Surface morphology of the films were studied by field emission scanning electron microscopy (SEM) using a JSM-7401F, operated at 3–5 kV.

Film's thickness was determined from near normal reflectance spectra, using a F-20 UV optical fibre reflectance spectrophotometer in contact probe mode.

Results and discussion

Composition and characteristics of growth: Composition of the samples was verified by EDS analysis. Film stoichiometry was close to ideal ZnO, and doped films maintain approximately the same Co/Zn ratio in film as in solution.

Fig. 1a shows the variation of deposition rate with film's thickness for undoped samples obtained at 673 and 723K, it is shown a linear increase of the deposition rate with thickness. The slope of this curve was almost the same for samples obtained at 723K and those obtained at 673 K. In addition, as expected the deposition rate at 723K was larger than that at 673K; the starting deposition rate (for thickness 0) was 53% larger at 723 K. Starting deposition rate was obtained from the intercept of the linear fit of deposition rate as a function of thickness. The increase of deposition rate with film's thickness can be explained by an increase of the nucleation centers as the film's thickness increase due to a change of the growing film texture (see below). Also, by the

<https://cimav.repositorioinstitucional.mx/jspui/>

change of the physical and chemical interaction between reactants and the surface, initially the substrate then the growing film [9]. In contrast, doped samples present a deposition rate nearly invariable with thickness, as it can be deduced from data in Table 1.

Table 1

Principal deposition conditions of films analyzed in this work. It is also tabulated the thickness (nm), deposition rate (nm min^{-1}), RMS roughness (nm) and average grain size (nm).

Sample	Co [at.%]	T_s [K]	Deposition time [min]	Thickness [nm]	Deposition rate [nm min^{-1}]	RMS roughness [nm]	Average grain size [nm]
A	0	723	64.0	763	11.9	29	235
B	0	723	54.0	365	6.8	14	219
C	0	723	36.5	188	5.2	16	188
D	0	723	29.9	166	5.5	-	-
E	0	723	14.1	70	5.0	-	-
F	0	673	69.0	419	6.1	15	210
G	0	673	52.5	334	6.4	9	81
H	0	673	38.7	163	4.2	-	-
I	0	673	37.0	122	3.3	-	-
J	0	673	37.0	101	2.7	18	165
K	0	623	75.0	101	1.3	14	111
DA	5	723	109.5	734	6.7	27	243
DB	5	723	73	409	5.6	12	166
DC	5	723	17	110	6.5	14	110
DD	10	723	65	624	9.6	27	210
DE	10	723	37.5	321	8.6	18	190
DF	10	723	17	173	10.2	19	88
DG	5	673	112.5	482	4.3	7	60
DH	5	673	73	322	4.4	8	118
DI	5	673	73	292	4.0	15	132
DJ	10	673	67	426	6.4	15	135
DK	10	673	32	208	6.5	3	159
DL	10	673	17.5	95	5.4	-	-

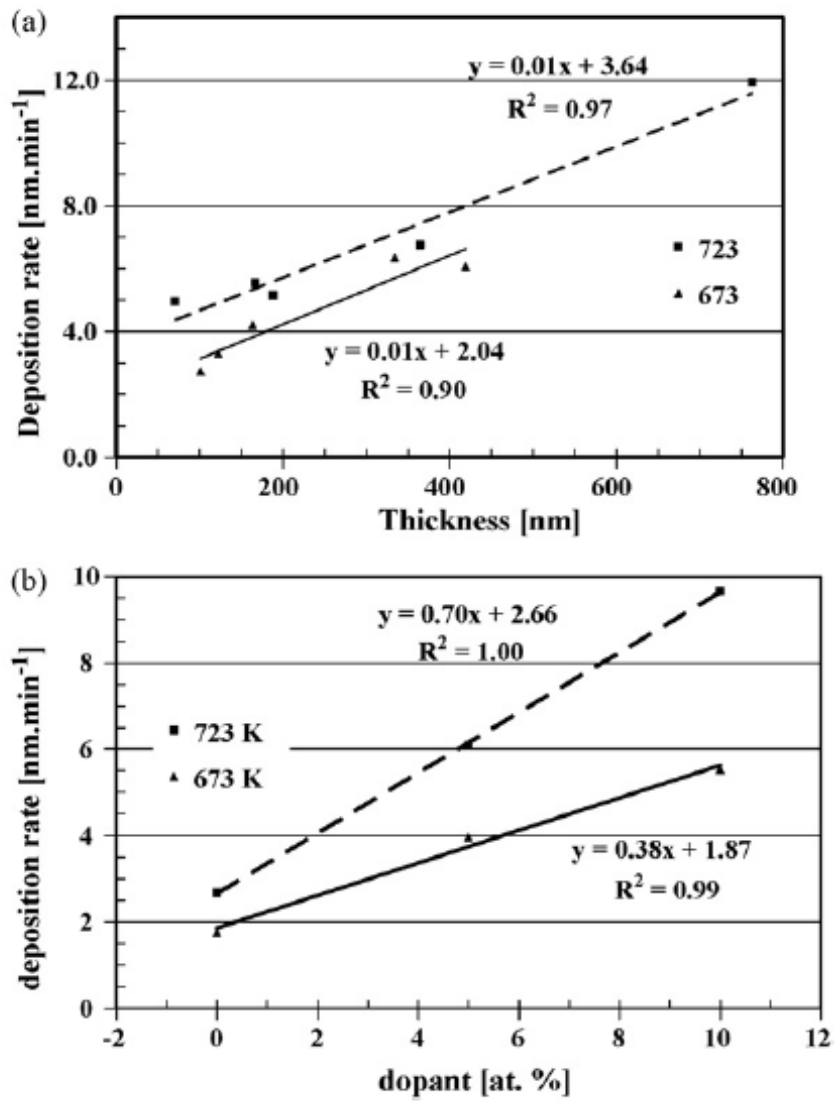


Fig. 1. (a) Deposition rate as a function of film's thickness for undoped samples obtained at 723 and 673 K. (b) Starting deposition rate as a function of Co concentration for films obtained at 673 and 723 K. Lines are least-squares fitting.

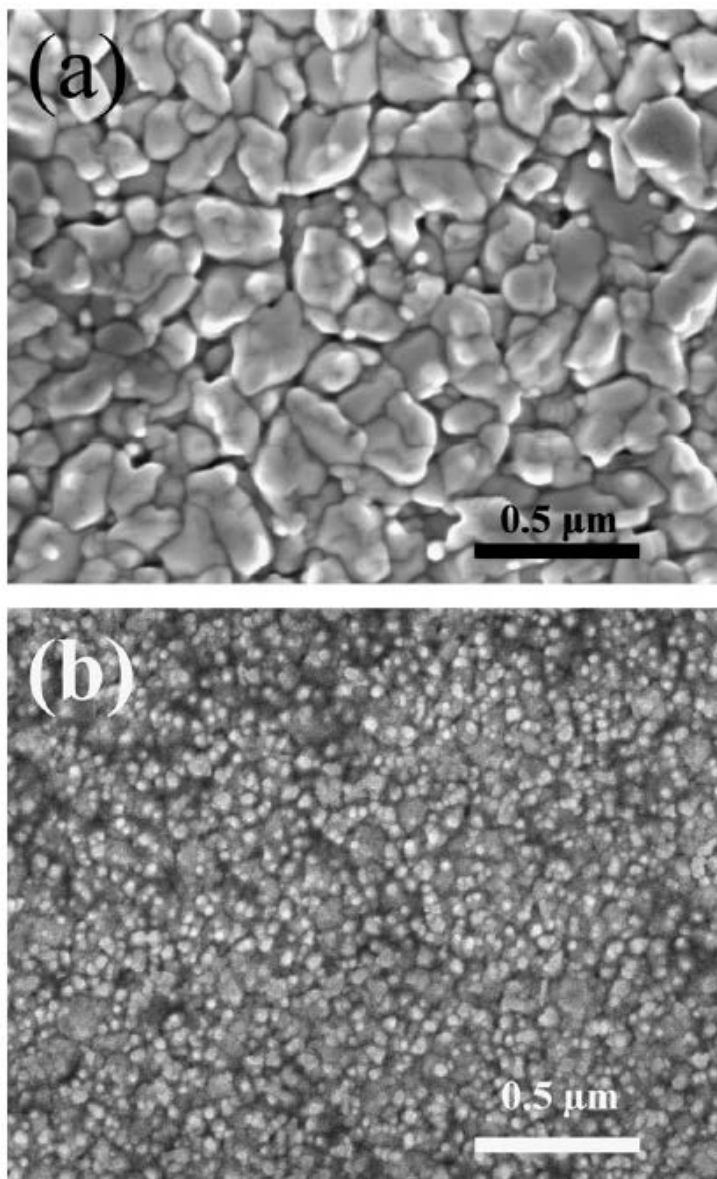


Fig. 2. SEM micrographs of undoped (a) and doped film with 5 at.% of Co (b).

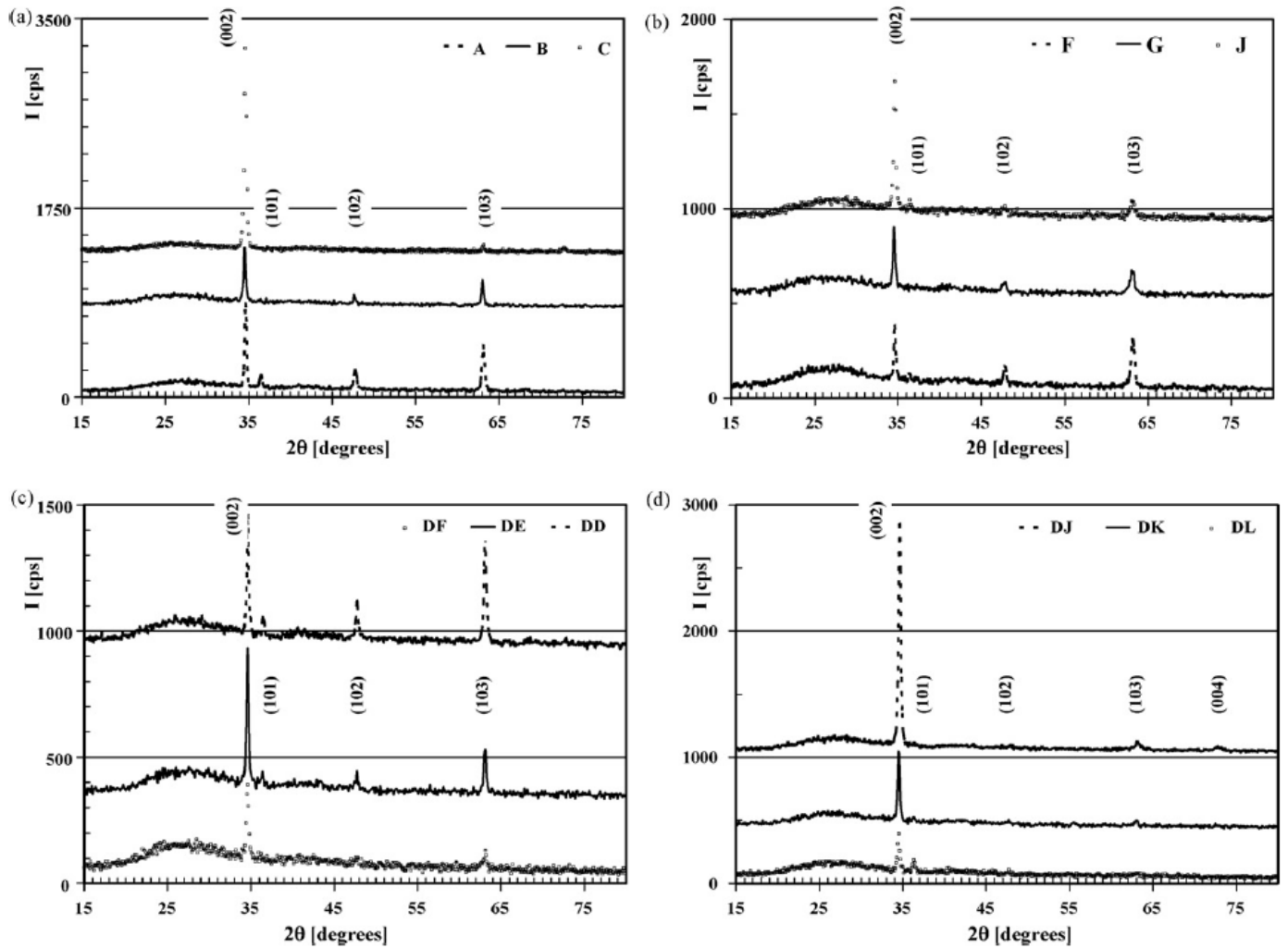


Fig. 3. X-ray diffraction patterns showing the influence of films' thickness. (a) Undoped samples obtained at 723 K. (b) Undoped samples obtained at 673 K. (c) Samples doped with 10% of Co, obtained at 723 K. (d) Samples doped with 10% of Co, obtained at 673 K.

However, the deposition rate for doped films was larger than that of undoped ones; also, it increased linearly with dopant content. Fig. 1b shows starting deposition rate as a function of Co concentration for films obtained at 673 and 723K. It is well established that thin film deposits form by a nucleation and growth mechanism [10]; and, that the rate-limiting step for nucleation processes on smooth surfaces is usually the formation of small clusters [11]. In addition, the presence of dopants can result in both the formation and stabilization of an equi-axed structure, with an increased formation of small clusters [10]. Then, the increase of deposition rate with dopant concentration can be explained by the creation of new nucleation centers as the dopant concentration increase, as reported for In doped films [9]. SEM analysis shows a clear tendency of grain size decrease with the addition of Co into the film (see Fig. 2). The grain size decrease can be correlated with the generation of more nucleation centers during the growth of the Co doped film. Up to 10 at.% of Co any decrease of growth rate was observed, in contrast to the case of other dopants reported elsewhere [12]; this difference can be explained by the very high solid solubility of CoO in Wurtzite ZnO, that can be metastably extended up to 40 at.% [13].

Microstructure: All the films were polycrystalline, single phase with a structure of Wurtzite type [14]. No other phases corresponding to metallic Co, other oxides or compounds were detected.

The influence of film's thickness was assessed for fixed deposition temperature and dopant concentration. For undoped films obtained at 673 and 723K, X-ray diffraction pattern results show that the texture of the films changes as the thickness

<https://cimav.repositorioinstitucional.mx/jspui/>

increase. It can be observed in Fig. 3 that undoped films, C and F of 188 and 101 nm of thickness, respectively, have a marked (0 0 2) texture; nevertheless the texture diminishes for thicker films (see Fig. 3a and b). Doped films deposited at 723K with 5 and 10 at.% of Co, showed the same tendency. Fig. 3c shows the correspondent diffraction pattern of films obtained at 723K with 10 at.% of Co. However, doped films grew at 673K showed small variation in their texture, but the opposite trend, i.e. an increase of the texture with the thickness of the films; as it can be seen in Fig. 3d for films with 10 at.% of dopant.

On the other hand, any influence of deposition temperature and dopant concentration onto the crystalline structure of the films was found considering films of almost the same thickness. Fig. 4 shows the diffraction pattern of undoped films of around 140 ± 40 nm of thickness obtained at different temperatures; all the films present a clear (0 0 2) texture. Diffraction pattern of films obtained at 723K with thickness around 365 ± 45 nm are shown in Fig. 4b; the samples have certain (0 0 2) preferred orientation, but any significant change in the texture can be noticed.

It is worthwhile to mention that comparison of the microstructure or properties of the films should be made on films of similar thickness, because many characteristics of the films depend on their thickness.

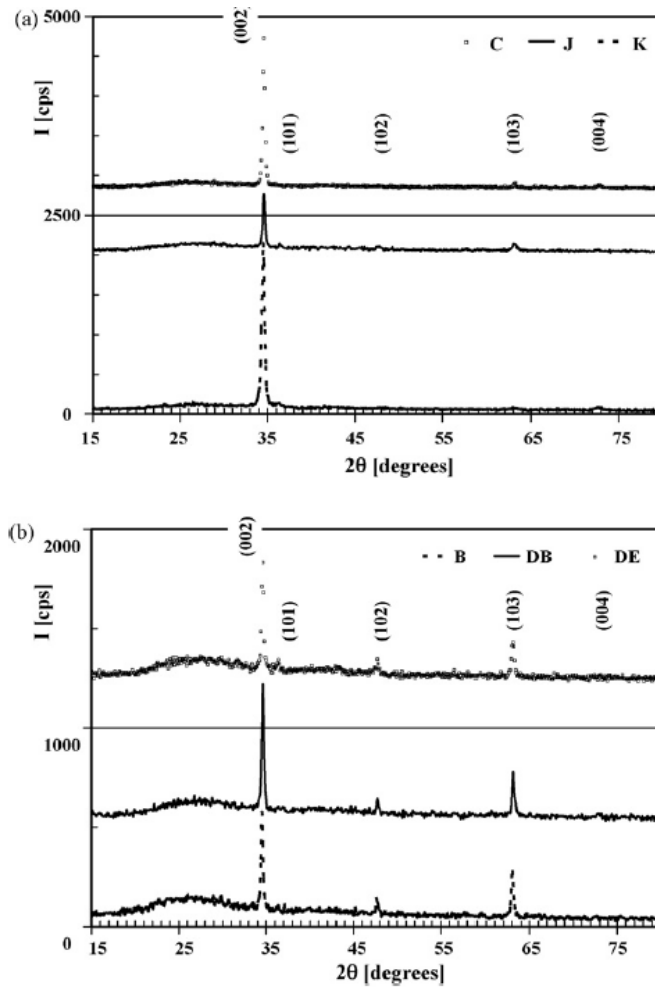


Fig. 4. X-ray diffraction patterns of films of similar thickness. (a) Showing the influence of deposition temperature for undoped samples (140 ± 40 nm); and (b) as a function of dopant concentration for samples obtained at 723 K (365 ± 44 nm).

Average grain size was estimated from measurement of several AFM images of the surface of the films. As expected, in general for undoped and doped samples, a clear tendency of grain size increase with the increase of film thickness and deposition temperature was noticed (see Table 1). Another interesting correlation was that films with strong (0 0 2) texture have small grain size, irrespective of the film's thickness or dopant concentration (see Table 1).

<https://cimav.repositorioinstitucional.mx/jspui/>

Surface rms roughness was also measured from a number of AFM images. Here also, the rms roughness increases as the film's thickness increases (see Table 1).

Acknowledgements

This work was partially supported by a grant from CONACYT SEP-47911.

Thanks to E. Torres-Moye, K. Campos, D. Lardizabal, S. Miranda, M. Moreno for their technical assistance.

References

- [1] J.M.D. Coey, *Curr. Opin. Solid State Mater. Sci.* 10 (2006) 83–92.
- [2] J.F. Gregg, I. Petej, E. Jouguelet, C. Dennis, *J. Phys. D: Appl. Phys.* 35 (2002) R121–R155.
- [3] T. Yamamoto, *Thin Solid Films* 420–421 (2002) 106.
- [4] J.H. Kim, H. Kim, D. Kim, Y.E. Ihm, W.K. Choo, *J. Appl. Phys.* 92 (2002) 6066.
- [5] H.J. Lee, S.Y. Jeong, C.R. Cho, C.H. Park, *Appl. Phys. Lett.* 81 (2002) 4020.
- [6] S.W. Lim, S.K. Hwang, J.M. Myoung, *Solid State Commun.* 125 (2003) 231.
- [7] V. Jayaram, J. Rajkumar, B.S. Rani, *J. Am. Ceram. Soc.* 82 (1999) 473.
- [8] F. Paraguay, D.W. Estrada, L.D.R. Acosta, E. Andrade, M. Miki-Yoshida, *Thin Solid Films* 350 (1999) 192–202.
- [9] D.J. Goyal, Ch. Agashe, M.G. Takwale, V.G. Bhide, S. Mahamuni, S.K. Kulkarni, *J. Mater. Res.* 8 (5) (1993) 1052.
- [10] W.A. Bryant, *J. Mater. Sci.* 12 (1977) 1285–1306.
- [11] J.A. Venables, G.D.T. Spiller, M. Hanbucken, *Rep. Prog. Phys.* 47 (1984) 399–459.
- [12] F. Paraguay, D.J. Morales, W. Estrada, E. Andrade, M. Miki-Yoshida, *Thin Solid Films* 366 (2000) 16.

<https://cimav.repositorioinstitucional.mx/jspui/>

[13] A. Tobias, Schaedlera, S.G. Ashutosh, M. Saito, M. Rühle, R. Gambino, C.G. Levi,
J. Mater. Res. 21 (3) (2006) 791.

[14] Joint Committee on Powder Diffraction Standards, Powder Diffraction File,
International Center for Diffraction Data, Swarthmore, PA, 1996, card 36-1451.